The Role of an Extra Fragment of Cytochrome *b* (Residues 309−326) in the Cytochrome bc_1 Complex from *Rhodobacter sphaeroides*†

Xing Gong, Linda Yu, and Chang-An Yu*

Department of Biochemistry and Molecular Biology, Oklahoma State University, Stillwater, Oklahoma 74078

Received June 1, 2006; Revised Manuscript Received July 27, 2006

ABSTRACT: In bacterial cytochrome *b* of the cytochrome bc_1 complex, there is an extra fragment located between the amphipathic helix *ef* and the transmembrane helix F compared to the mitochondrial counterparts. In this work, mutants at various positions of this extra fragment were generated in *Rhodobacter sphaeroides* in an effort to investigate its specific role in the bacterial bc_1 complex. The total deletion [cyt*b*-Δ(309−326)] and alanine substitution [cyt*b*-(309−326)A] mutant complexes have about 20% of the bc_1 activity found in the wild-type complex. Mutant complexes of cyt*b*-(309−311)A, cyt*b*-(312−314)A, cyt*b*-(315−317)A, cyt*b*-(318−321)A, cyt*b*-(322−323)A, cyt*b*-(324−326)A, cyt*b*-(F323A), and cyt*b*-(S322A) have respectively 87%, 85%, 89%, 100%, 32%, 90%, 100%, and 32% of the bc_1 activity, indicating that the S322 of cytochrome *b* is important. EPR spectral analysis reveals that the [2Fe-2S] cluster in the cyt*b*-(S322A) mutant complex has a broadened and shifted g_x signal ($g = 1.76$). The rate of superoxide anion ($O_2^{\bullet-}$) generation is 4 times higher in the cyt*b*-(S322A) mutant complex than in the wild-type or mutant complexes of S322T, S322Y, or S322C. These results support the idea that alanine substitution at S322 of cytochrome *b* causes conformational changes at the Q_o site by weakening the binding between cytochrome *b* and ISP through hydrogen bonding provided by the hydroxyl group of this residue. This change facilitates electron leakage from the Q_o site for reaction with molecular oxygen to form superoxide anion, thus decreasing bc_1 activity.

The cytochrome bc_1 complex (also known as ubiquinol−cytochrome *c* reductase or complex III) is an essential segment of mitochondrial and most bacterial respiratory electron transport chains (*1*). This complex catalyzes electron transfer from ubiquinol to cytochrome *c* (c_2 in bacteria) and concomitantly translocates protons across the membrane to generate a membrane potential and pH gradient for ATP synthesis.

All of the cytochrome bc_1 complexes contain three core subunits: cytochrome *b* (with two *b*-type hemes, b_L and b_H), cytochrome c_1 (with one *c*-type heme, c_1), and Rieske iron−sulfur protein (ISP)[1] with a high potential [2Fe-2S] cluster. The cytochrome *b* subunit also houses two ubiquinone binding sites, the ubiquinol oxidation site (Q_o) and the ubiquinone reduction site (Q_i). In addition to three core subunits, cytochrome bc_1 complexes from different sources process a varying number of supernumerary subunits (*2*, *3*). For example, complexes from bovine heart mitochondria, yeast, *Rhodobacter sphaeroides*, and *Rhodobacter capsulatus* have respectively eight, seven, one, and no supernumerary subunits. The electron transfer activity and stability of the cytochrome bc_1 complex seem to have a direct correlation with the number of supernumerary subunits present since the complexes containing no supernumerary subunit have lower activity and are less stable than those with a supernumerary subunit (*2*).

The core subunits in bacterial complexes are generally bigger than their counterparts in the mitochondrial complexes. Sequence alignment of bacterial cytochrome *b*, cytochrome c_1, and ISP with their counterparts in the mitochondrial complexes reveals four extra fragments in bacterial cytochrome *b* and one each in bacterial ISP and cytochrome c_1 (*4*). In the structure model of the *R. sphaeroides* cytochrome bc_1 complex (*4*), these four extra fragments of cytochrome *b* are located (1) at the N-terminus (residues 2−12), (2) at the connecting loop between helices D and E (residues 232−239), (3) at the connecting loop between *ef* and F (residues 309−326), and (4) at the C terminus (residues 421−445). The extra fragment of cytochrome c_1 (residues 141−161) is located at the long loop after helix α-3, and the extra fragment of ISP (residues 96−107), which forms an α-helical structure, is located near the middle portion of the subunit. The recently available, low-resolution X-ray crystal structure of the *R. capsulatus* bc_1 complex (*5*) reveals that the positions of these extra fragments are at the same positions as those of *R. sphaeroides*. Unfortunately, the diffraction densities at these extra fragments are very poor, and no detailed structural information is revealed.

† This work was supported by Grants GM30721 (to C.-A.Y.) from the National Institutes of Health and MCB0077650 (to L.Y.) from National Science Foundation and the Oklahoma Agricultural Experiment Station (Projects 1819 and 2372), Oklahoma State University.

* Corresponding author. Phone: (405) 744-6612. Fax: (405) 744-6612. E-mail: cayuq@okstate.edu.

[1] Abbreviations: cyt, cytochrome; DSC, differential scanning calorimetry; DM, *n*-dodecyl β-D-maltoside; EPR, electron paramagnetic resonance; [2Fe-2S], Rieske iron−sulfur center; ISP, Rieske iron−sulfur protein; MCLA, 2-methyl-6-(4-methoxyphenyl)-3,7-dihydroimidazolyl-[1,2-*a*]pyrazin-3-one hydrochloride; $O_2^{\bullet-}$, superoxide anion; PAGE, polyacrylamide gel electrophoresis; $Q_0C_{10}BrH_2$, 2,3-dimethoxy-5-methyl-6-(10-bromodecyl)-1,4-benzoquinol; SOD, superoxide dismutase; SDS, sodium dodecyl sulfate; XO, xanthine oxidase.

10.1021/bi061099a CCC: $33.50
Published on Web 08/26/2006

Are these extra fragments required for the bc_1 complex? One way to answer this question is to systematically mutate residues in these extra fragments and to determine the stability and function of the resulting mutant complexes. By using this approach, the ISP extra fragment is found to be required for structural stability of ISP in the complex (*6*), and the C-terminal extra fragment of cytochrome *b* is essential for maintaining the structural integrity of the complex (*7*). However, knowledge of the role of other extra fragments of cytochrome *b* in the *R. sphaeroides* bc_1 complex is still lacking.

The third extra fragment of cytochrome *b* (residues 309−326 in *R. sphaeriodes*) is in close proximity to the Q_o site where the bifurcated oxidation of ubiquinol is carried out according to the "protonmotive Q-cycle" mechanism (*8*). At the Q_o site, one electron from ubiquinol is transferred to the ISP and then to cytochrome c_1, while the other electron is transferred to cytochrome b_L and then cytochrome b_H. It has been reported that, during the electron transfer through the bc_1 complex, the second electron of ubiquinol at the low-potential chain can react with molecular oxygen to form superoxide anion ($O_2^{\bullet -}$) (*9*−*13*). The electron leakage site has been thought to be located at the reduced cytochrome b_L or ubisemiquinone of the Q_o site. Studies on the role of the third extra fragment in *R. sphaerodies* cytochrome *b* may help us to understand structural elements involved in structural stability of the Q_o site and thus to understand the bc_1 complex function.

Herein we report the generation of *R. sphaeroides* mutants expressing His-tagged cytochrome bc_1 complexes with deletion or substitution at various positions in the third extra fragment of cytochrome *b* to investigate the role of this fragment in the complex. The photosynthetic growth behavior, the bc_1 activity, and the amount of cytochrome *b*, cytochrome c_1, ISP, and subunit IV in the chromatophore membrane and in the purified complex of the wild type and mutants were determined and compared in order to identify the critical amino acid residue(s). The effect of mutations on EPR spectra of ISP and on superoxide anion generation during ubiquinol oxidation by the complex was also examined.

EXPERIMENTAL PROCEDURES

Materials. Cytochrome *c* (horse heart, type III), hypoxanthine, superoxide dismutase (SOD), and xanthine oxidase were purchased from Sigma Chemical Co. *n*-Dodecyl β-D-maltoside (DM) and *n*-octyl β-D-glucoside were from Anatrace. Nickel nitrilotriacetic acid (Ni-NTA) gel and a Qiaprep spin Miniprep kit were from Qiagen. 2-Methyl-6-(4-methoxyphenyl)-3,7-dihydroimidazolyl[1,2-*a*]pyrazin-3-one hydrochloride (MCLA) was from Molecular Probes, Inc. 2,3-Dimethoxy-5-methyl-6-(10-bromodecyl)-1,4-benzoquinol ($Q_0C_{10}BrH_2$) was prepared in our laboratory as previously reported (*14*). All other chemicals were of the highest purity commercially available.

Growth of Bacteria. Escherichia coli cells were grown at 37 °C in LB medium. Extra rich media, e.g., TYP (1.6 g of Bact-tryptone, 1.6 g of Bacto-yeast extract, 0.5 g of NaCl, and 0.25 g of K_2HPO_4 in 100 mL of medium), were used in procedures for the rescue of single-stranded DNA or the purification of low copy number plasmids (*15*). For photosynthetic growth of the plasmid-bearing *R. sphaeroides* BC17 cells, an enriched Siström's medium containing 5 mM glutamate and 0.2% casamino acids was used. Photosynthetic growth conditions for *R. sphaeroides* were essentially as described previously (*16*). Cells harboring the mutated cytochrome *b* gene on the pRKD418-*fbc*FB_mC_HQ plasmid were grown photosynthetically for one or two serial passages to minimize any pressure for reversion. The inoculation volumes used for photosynthetic cultures were at least 5% of the total volume. Antibiotics were added to the following concentrations: ampicillin (125 μg/mL), kanamycin sulfate (30 μg/mL), tetracycline (10 μg/mL for *E. coli* and 1 μg/mL for *R. sphaeroides*), and trimethoprim (100 μg/mL for *E. coli* and 30 μg/mL for *R. sphaeroides*).

Generation of R. sphaeroides Strains Expressing the His_6-Tagged Cytochrome bc_1 Complexes with Mutations at the Extra Fragment of Cytochrome b (Residues 309−326). Mutations were constructed by site-directed mutagenesis using the Altered Sites II mutagenesis system from Promega or the QuikChange site-directed mutagenesis kit from Stratagene. The cyt*b*-(309−326)A mutant was constructed by the Altered Sites II mutagenesis method using single-stranded pSELNB3503 (*17*) as template and the following mutant oligonucleotide as the annealing primer, 5′-GCGATCCTGCGCGCCTTGCCGCCGCCGCCGCCGCCGCCGCCGCCGCCGCCGCCGCCGCCGCCGCCGCCGCCCGACGCCAAGTTCT-3′. The underlined bases correspond to the genetic codes for the target mutated amino acids. Other mutants were constructed by the QuikChange site-directed mutagenesis method using a supercoiled double-stranded pGEM7Zf(+)-*fbc*FB as template and a forward and a reverse primer for PCR amplification. The pGEM7Zf(+)-*fbc*FB plasmid (*6*) was constructed by ligating the *Eco*RI−*Xba*I fragment from pSELNB3503 into *Eco*RI and *Xba*I sites of the pGEM7Zf-(+) plasmid. The primers used are given in Table 1.

Following mutagenesis, a 962 base pair *Bst*EII−*Xba*I fragment from pSELNB3503 or pGEM7Zf(+)-*fbc*FB plasmid containing the mutant cytochrome *b* gene was ligated into *Bst*EII and *Xba*I sites of the low copy number plasmid, pRKD418-*fbc*FB_{KmBX}CHQ, to generate the pRKD418-*fbc*FB_mCHQ plasmid. Loss of kanamycin resistance was then used to screen for recombinant plasmids. A plate-mating procedure (*16*) was used to mobilize the pRKD418-*fbc*FB_m-CHQ plasmid in *E. coli* S17-1 cells into *R. sphaeroides* BC17 cells. The presence of engineered mutations was confirmed by DNA sequencing of the 962 base pair *Bst*EII−*Xba*I fragment before and after photosynthetic growth of the cells as previously reported (*16*). DNA sequencing and oligonucleotide syntheses were performed by the Recombinant DNA/Protein Core Facility at Oklahoma State University.

Enzyme Preparations and Activity Assay. Chromatophores were prepared, from which the His_6-tagged cytochrome bc_1 complexes were purified, as previously reported (*17*). Quantification of the bc_1 complexes was performed according to published methods using extinction coefficients of 28.5 mM^{-1} cm^{-1} at 563−578 nm for cytochrome *b* (*18*) and 17.5 mM^{-1} cm^{-1} at 553−539 nm for cytochrome c_1 (*19*). To assay ubiquinol−cytochrome *c* reductase activity, chromatophores or purified cytochrome bc_1 complexes were diluted with 50 mM Tris-HCl, pH 8.0, containing 200 mM NaCl and 0.01% dodecyl maltoside (DM) to a final concentration of cytochrome *b* of 3 μM. Appropriate amounts of the diluted

Table 1: Oligonucleotides Used for Site-Directed Mutagenesis[a]

cyt*b*Δ-(309−326) (F)	5′-CCTTCTACGCGATCCTGCGCGCCTTCGACGCCAAGTTCTTCGGCGTG-3′
cyt*b*Δ-(309−326) (R)	5′-CACGCCGAAGAACTTGGCGTCGAAGGCGCGCAGGATCGCGTAGAAGG-3′
cyt*b*-(309−311)A (F)	5′-CTGCGCGCCTTCGCCGCCGCCGTCTGGGT GGTGCAGATCGCCAAC-3′
cyt*b*-(309−311)A (R)	5′-GTTGGCGATCTGCACCACCCAGACGGCGGCGGCGAAGGCGCGCAG-3′
cyt*b*-(312−314)A (F)	5′-GCCTTCACCGCCGACGCCGCGGCGGTGCAGATCGCCAAC-3′
cyt*b*-(312−314)A (R)	5′-GTTGGCGATCTGCACCGCCGCGGCGTCGGCGGTGAAGGC-3′
cyt*b*-(315−317)A (F)	5′-CCGCCGACGTCTGGGTGGCCGCCGCCGCCAACTTCATCAGCTTC-3′
cyt*b*-(315−317)A (R)	5′-GAAGCTGATGAAGTTGGCGGCGGCGGCCACCCAGACGTCGGCGG-3′
cyt*b*-(318−321)A (F)	5′-GGGTGGTGCAGATCGCCGCCGCCGCCAGCTTCGGCATC-3′
cyt*b*-(318−321)A (R)	5′-GATGCCGAAGCTGGCGGCGGCGGCGATCTGCACCACCC-3′
cyt*b*-(322−323)A (F)	5′-CGCCAACTTCATCGCCGCCGGCATCATCGACGCCAAGTTCTTC-3′
cyt*b*-(322−323)A (R)	5′-GAAGAACTTGGCGTCGATGATGCCGGCGGCGATGAAGTTGGCG-3′
cyt*b*-(324−326)A (F)	5′-GCCAACTTCATCAGCTTCGCCGCCGCCGACGCCAAGTTCTTC-3′
cyt*b*-(324−326)A (R)	5′-GAAGAACTTGGCGTCGGCGGCGGCGAAGCTGATGAAGTTGGC-3′
cyt*b*-(S322A) (F)	5′-CGCCAACTTCATCGCCTTCGGCATCATCGACGCCAAG-3′
cyt*b*-(S322A) (R)	5′-CTTGGCGTCGATGATGCCGAAGGCGATGAAGTTGGCG-3′
cyt*b*-(F323A) (F)	5′-GCCAACTTCATCAGCGCCGGCATCATCGACGCCAAG-3′
cyt*b*-(F323A) (R)	5′-CTTGGCGTCGATGATGCCGGCGCTGATGAAGTTGGC-3′
cyt*b*-(S322T) (F)	5′-CGCCAACTTCATCACCTTCGGCATCATCGACGCCAAG-3′
cyt*b*-(S322T) (R)	5′-CTTGGCGTCGATGATGCCGAAGGTGATGAAGTTGGCG-3′
cyt*b*-(S322C) (F)	5′-CGCCAACTTCATCTGCTTCGGCATCATCGACGCCAAG-3′
cyt*b*-(S322C) (R)	5′-CTTGGCGTCGATGATGCCGAAACGGATGAAGTTGGCG-3′
cyt*b*-(S322Y) (F)	5′-CGCCAACTTCATCTACTTCGGCATCATCGACGCCAAG-3′
cyt*b*-(S322Y) (R)	5′-CTTGGCGTCGATGATGCCGAAATGGATGAAGTTGGCG-3′
cyt*b*-(S322V) (F)	5′-CGCCAACTTCATCGTCTTCGGCATCATCGACGCCAAG-3′
cyt*b*-(S322V) (R)	5′-CTTGGCGTCGATGATGCCGAACAGGATGAAGTTGGCG-3′
cyt*b*-(S322L) (F)	5′-CGCCAACTTCATCCTCTTCGGCATCATCGACGCCAAG-3′
cyt*b*-(S322L) (R)	5′-CTTGGCGTCGATGATGCCGAAGAGGATGAAGTTGGCG-3′
cyt*b*-(S322I) (F)	5′-CGCCAACTTCATCATCTTCGGCATCATCGACGCCAAG-3′
cyt*b*-(S322I) (R)	5′-CTTGGCGTCGATGATGCCGAATAGGATGAAGTTGGCG-3′
cyt*b*-(S322F) (F)	5′-CGCCAACTTCATCTTCTTCGGCATCATCGACGCCAAG-3′
cyt*b*-(S322F) (R)	5′-CTTGGCGTCGATGATGCCGAAAAGGATGAAGTTGGCG-3′

[a] F and R in parentheses denote forward and reverse primers, respectively. The underlined bases correspond to the genetic codes for the amino acid(s) to be mutated.

samples were added to 1 mL of assay mixture containing 100 mM Na^+/K^+ phosphate buffer, pH 7.4, 300 μM EDTA, 100 μM cytochrome *c*, and 25 μM $Q_0C_{10}BrH_2$. Potassium cyanide (30 μM) was added to the assay mixture when bc_1 activity in chromatophores was determined. For determination of the apparent K_m for $Q_0C_{10}BrH_2$, various concentrations of $Q_0C_{10}BrH_2$ were used. Activities were determined by measuring the reduction of cytochrome *c* (the increase of absorbance at 550 nm) in a Shimadzu UV-2401 PC spectrophotometer at 23 °C, using a millimolar extinction coefficient of 18.5 for calculation. The nonenzymatic oxidation of $Q_0C_{10}BrH_2$, determined under the same conditions in the absence of enzyme, was subtracted from the assay.

Measurement of Superoxide Anion Generation. Superoxide anion ($O_2^{\bullet-}$) generation by the cytochrome bc_1 complex was determined by measuring the chemiluminescence of the MCLA−$O_2^{\bullet-}$ adduct in an Applied Photophysics stopped-flow reaction analyzer, SX.18MV (Leatherhead, England), by leaving the excitation light off and registering light emission, as described previously (*20*). Reactions were carried out at 23 °C by rapidly mixing 1:1 solutions A and B. Solution A contains 100 mM Na^+/K^+ phosphate buffer, pH 7.4, 1 mM EDTA, 1 mM KCN, 1 mM NaN_3, 0.1% BSA, 0.01% DM, and an appropriate amount of the wild-type or mutant bc_1 complex. Solution B was the same as solution A except with bc_1 complex being replaced with 50 μM $Q_0C_{10}BrH_2$ and 4 μM MCLA. $O_2^{\bullet-}$ generation is expressed in XO units. One XO unit is defined as chemiluminescence (maximum peak height of light intensity) generated by 1 unit of xanthine oxidase, which equals 2.71 V in an Applied Photophysics stopped-flow reaction analyzer, SX.18MV, when solution A containing 100 mM Na^+/K^+ phosphate buffer, pH 7.4, 100 μM hypoxanthine, 4 μM MCLA, and 1 mM NaN_3 is mixed with solution B containing 100 mM Na^+/K^+ phosphate buffer, pH 7.4, 1 mM NaN_3, and 50 units/mL xanthine oxidase.

Differential Scanning Calorimetry. Calorimetric measurements were performed with a CSC 6100 NanoII DSC. The reference and sample solutions were degassed under vacuum for 15 min prior to use. A 0.50 mL bc_1 solution, 2 mg/mL, in 50 mM K^+/Na^+ phosphate buffer, pH 7.4, containing 100 mM KCl and 0.002% DM was placed in the sample capillary cell, and the same amount of buffer was placed in the reference capillary cell. All DSC scans reported in this study were run at a rate of 1 °C/min. After the first scan, the samples were cooled to the original temperature and rescanned. Since after the first scan the protein was completely and irreversibly denatured, no thermotransition peaks were observed in the second scan. Thus the second scan could be used as a baseline. All thermodynamic analyses were carried out according to the program known as CpCal from the Nano DSC program group.

Other Biochemical and Biophysical Techniques. Ubiquinone content was determined according to the procedure reported by Redfearn (*21*). Protein concentration was determined by the method of Lowry et al. (*22*). SDS−PAGE was performed according to Laemmli (*23*) using a Bio-Rad Mini-Protean dual slab vertical cell. Samples were denatured with 10 mM Tris-HCl buffer, pH 6.8, containing 1% SDS and 3% glycerol in the presence of 0.4% β-mercaptoethanol for 2 h at 37 °C before being subjected to electrophoresis. Western blotting was performed with rabbit polyclonal

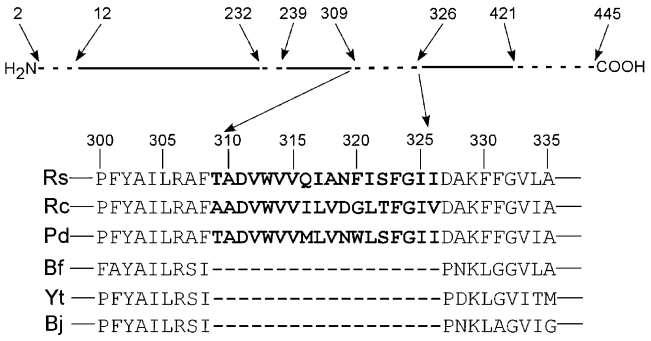

FIGURE 1: Partial sequence comparison in the third extra fragment of various cytochromes *b*. Abbreviations: RS, *R. sphaeroides*; RC, *R. capsulatus*; Pd, *Paracoccus denitrificans*; Bf, beef; Yt, yeast; Bj, *Bradyrhizobium japonicum*.

antibodies against cytochrome *b*, cytochrome c_1, ISP, and subunit IV of the *R. sphaeroides* bc_1 complex (*20*). The polypeptides separated by SDS−PAGE gel were transferred to polyvinylidene difluoride membrane for immunoblotting. Goat anti-rabbit IgG conjugated to alkaline phosphatase or protein A conjugated to horseradish peroxidase was used as the second antibody.

Redox titrations of cytochromes *b* and c_1 in complement and mutant bc_1 complexes were conducted potentiometrically according to the previously published method (*24*, *25*) using a Shimadzu model UV-2410 spectrophotometer. Aliquots (3 mL) of the bc_1 complex (2 μM cytochrome *b*) in 0.1 M Na^+/K^+ phosphate buffer, pH 7.0, were used in the presence of 20 μM phenazine methosulfate, 20 μM phenazine ethosulfate, 20 μM phenazine, 20 μM pyocyanine, 25 μM 1,4-benzoquinone, 25 μM 1,2-naphthoquinone, 25 μM 1,4-naphthoquinone, 50 μM duroquinone, 70 μM 2,3,5,6-tetramethyl-*p*-phenylenediamine, and 15 μM 2-hydroxy-1,4-naphthoquinone as mediators. For oxidative titration, samples were first reduced by sodium dithionite and then titrated with potassium ferricyanide solution. For reductive titration, samples were first oxidized by ferricyanide and then titrated with sodium dithionite solution. The redox state of the [2Fe-2S] cluster was determined by circular dichroism using a JASCO J-715 spectropolarimeter (*26*, *27*). Instrument settings for the spectropolarimeter were as follows: scan speed, 100 nm/min; step resolution, 1 nm; accumulation, 10 traces for averaging; response, 1 s; bandwidth, 1.0 nm; sensitivity, 10 mdeg; and slit width, 500 μm.

Low-temperature EPR spectra were recorded with a Bruker EMX EPR spectrometer equipped with an Air Products flow cryostat. The instrument setting details are provided in the legend of the relevant figure.

RESULTS AND DISCUSSION

The Requirement of an Extra Fragment of Cytochrome b (Residues 309−326) for the Cytochrome bc_1 Complex. *R. sphaeroides* cytochrome *b* has an extra fragment that corresponds to residues 309−326 with a sequence of -TADVWVVQIANFISFGII- (see Figure 1). This fragment is located between the amphipathic helix *ef*, a key structural component of the Q_o site, and the transmembrane helix F of the cytochrome *b* (Figure 2) (*4*). To probe the role of this fragment, *R. sphaeroides* mutants expressing His_6-tagged bc_1 complexes with deletion or substitution at various positions of the extra fragment were generated and characterized.

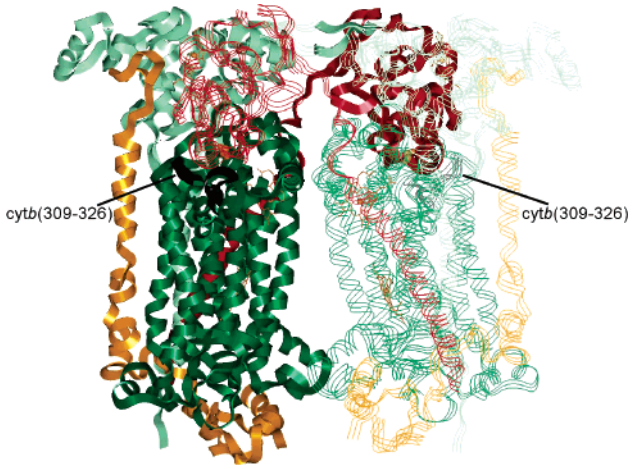

FIGURE 2: Location of an extra fragment of cytochrome *b* (residues 309−326) in the proposed structural model of the *R. sphaeroides* bc_1 complex. One monomer (left) is displayed in solid ribbons, and the symmetric monomer (right) is displayed in three-thread-line ribbons. Cytochrome c_1 is in silver, ISP is in brown, subunit IV is in rust, cytochrome *b* is in green, and the extra fragment (residues 309−326) is in black. The figure was prepared on a Silicon Graphics O2 work station using the commercially available Insight II software package (Accelrys Inc., San Diego, CA).

Table 2: Characterization of Mutants in Cytochrome *b* of the bc_1 Complex

mutant	photo-synthetic growth	bc_1 complex specific activity[a]	
		chromatophore	purified complex[b]
wild type	++[c]	2.21 ± 0.04	2.50 ± 0.04
cyt*b*-Δ(309−326)	+[d]	0.44 ± 0.03	0.53 ± 0.01
cyt*b*-(309−326)A	+	0.46 ± 0.04	0.52 ± 0.04
cyt*b*-(309−311)A	++	1.90 ± 0.02	2.18 ± 0.02
cyt*b*-(312−314)A	++	1.96 ± 0.03	2.13 ± 0.03
cyt*b*-(315−317)A	++	2.06 ± 0.04	2.23 ± 0.04
cyt*b*-(318−321)A	++	2.21 ± 0.02	2.49 ± 0.02
cyt*b*-(322−323)A	+	0.69 ± 0.01	0.80 ± 0.04
cyt*b*-(324−326)A	++	2.01 ± 0.04	2.25 ± 0.01
cyt*b*-(S322A)	+	0.68 ± 0.03	0.81 ± 0.04
cyt*b*-(F323A)	++	2.22 ± 0.04	2.52 ± 0.03
cyt*b*-(S322T)	++	2.21 ± 0.04	2.51 ± 0.02
cyt*b*-(S322C)	++	2.10 ± 0.02	2.45 ± 0.04
cyt*b*-(S322Y)	++	2.08 ± 0.04	2.43 ± 0.03
cyt*b*-(S322V)	+	0.68 ± 0.04	0.80 ± 0.03
cyt*b*-(S322L)	+	0.67 ± 0.03	0.81 ± 0.04
cyt*b*-(S322I)	+	0.68 ± 0.02	0.82 ± 0.03
cyt*b*-(S322F)	+	0.69 ± 0.04	0.81 ± 0.04

[a] Specific activity is expressed as micromoles of cytochrome *c* reduced per minute per nanomole of cytochrome *b* at room temperature. The data presented were mean values ± SD from four experiments. [b] The purified bc_1 complex was in 50 mM Tris-HCl, pH 8.0, containing 200 mM NaCl, 200 mM histidine, and 0.5% octyl glucoside. [c] ++, cell growth rate is essentially the same as that of the wild-type cells. [d] +, cells grow photosynthetically with a rate comparable to that of the complement cells after a lag period.

When this extra fragment of cytochrome *b* is deleted, the resulting cells [cyt*b*-Δ(309−326)] start to grow photosynthetically at a rate comparable to that of the wild-type cells after a long lag time. Chromatophores prepared from this mutant have only 20% of the bc_1 activity found in the wild-type chromatophores (see Table 2). A similar electron transfer activity is found in the bc_1 complex purified from chromatophores of this mutant (see Table 2). These results indicate that this region is required for optimal bc_1 complex activity.

To further confirm that a decrease in bc_1 activity found in the [cyt*b*-Δ(309−326)] mutant complex results from the essentiality of this extra fragment, and not from improper protein assembly or folding due to the large deletion, a mutant with this extra fragment substituted with alanine [cyt*b*-(309−326)A] was generated and characterized. This mutant cell has photosynthetic growth behavior and bc_1 activity similar to those of the cyt*b*-Δ(309−326) mutant. These results indicate that this extra fragment of cytochrome *b* is required for bacterial cytochrome bc_1 complex activity.

Serine-322 Is an Important Residue in This Extra Fragment of Cytochrome b. To identify critical amino acid residues in this extra fragment, we first located the critical regions. Residues in six portions of this fragment were replaced with alanine to generate six mutants, cyt*b*-(309−311)A, cyt*b*-(312−314)A, cyt*b*-(315−317)A, cyt*b*-(318−321)A, cyt*b*-(322−323)A, and cyt*b*-(324−326)A. When these mutants were subjected to photosynthetic growth conditions, mutants cyt*b*-(309−311)A, cyt*b*-(312−314)A, cyt*b*-(315−317)A, cyt*b*-(318−321)A, and cyt*b*-(324−326)A grew photosynthetically at rates comparable with that of the wild-type cells. However, the cyt*b*-(322−323)A mutant has a longer lag time (>12 h) before it starts to grow at a rate comparable to that of the wild-type cells. This growth behavior is similar to that of mutants [cyt*b*-Δ(309−326)] and [cytb-(309−326)A]. Chromatophores prepared from mutants cyt*b*-(309−311)A, cyt*b*-(312−314)A, cyt*b*-(315−317)A, cyt*b*-(318−321)A, and cyt*b*-(324−326)A have respectively 86%, 89%, 93%, 100%, and 91% of the bc_1 activity detected in the wild-type chromatophores. Similar activities are observed in bc_1 complexes purified from these mutant chromatophores (see Table 2). On the other hand, chromatophores and the purified complex obtained from the cyt*b*-(322−323)A mutant have only 31% of the bc_1 activity found in the wild-type chromatophores or the bc_1 complex. These results indicate that either one or both residues 322 and 323 of cytochrome *b* are important.

Since residues 322 and 323 of cytochrome *b* are Ser and Phe, to see which of these two residues is essential, mutants cyt*b*-(S322A) and cyt*b*-(F323A) were generated and characterized. As shown in Table 2, chromatophores prepared from these two mutants have respectively 31% and 100% of the bc_1 activity found in the wild-type chromatophores, indicating that S322 of cytochrome *b* is critical. The S322 is highly conserved in bacterial cytochromes *b*.

Importance of the Hydroxyl Group in the Ser-322 of Cytochrome b. Absorption spectral analysis reveals that the amounts and absorption properties of cytochromes *b* and c_1 in mutant complexes of cyt*b*-Δ(309−326), cyt*b*-(309−326)A, and cyt*b*-(S322A) are the same as those in the wild-type complex. Western blot analysis using antibodies against *R. sphaeroides* cytochrome *b*, cytochrome c_1, ISP, and subunit IV also indicates that these mutant complexes have the same amount of cytochrome *b*, cytochrome c_1, ISP, and subunit IV as does the wild-type complex. The redox midpoint potentials (E_m) of cytochromes *b* and c_1 in these mutant complexes are also the same as those in the wild-type complex [$E_{m(b_L)} = -87 \pm 6$ mV, $E_{m(b_H)} = 41 \pm 8$ mV, $E_{m(c_1)} = 237 \pm 6$ mV, and data on standard deviations (SD) of the midpoint potentials were obtained from four trials of titrations]. Thus, the decrease in bc_1 activity in the cyt*b*-(S322A) mutant complex is not due to mutational effects on the assembly of the bc_1 protein subunits into the chromatophore membrane or to a change of the redox potential of cytochromes *b* and c_1 in the complex.

Since S322 contains a hydroxyl group, it is possible that the loss of bc_1 activity in the cyt*b*-(S322A) mutant complex results from the mutation abolishing the hydrogen bond forming ability of the residue at this position. To confirm this possibility, mutants with S322 substituted with hydroxyl-containing residues [cyt*b*-(S322T) and cyt*b*-(S322Y)] or an SH-containing residue [cyt*b*-(S322C)] or non-hydroxyl-containing residues [cyt*b*-(S322V), cyt*b*-(S322L), cyt*b*-(S322I), and cyt*b*-(S322F)] were generated and characterized. These first three mutants [cyt*b*-(S322T), cyt*b*-(S322Y), and cyt*b*-(S322C)] grow photosynthetically at a rate comparable to that of the wild-type cells and, in bc_1 complexes in chromatophore membranes or in the purified state, have the same electron transfer activity as that of the wild-type complex (see Table 2). As expected, mutants cyt*b*-(S322V), cyt*b*-(S322L), cyt*b*-(S322I), and cyt*b*-(S322F) have photosynthetic growth behavior and bc_1 activity similar to those of the cyt*b*-(S322A) mutant. These results indicate that a hydrogen bond forming group at position 322 of cytochrome *b* is essential for the electron transfer activity of the bc_1 complex.

Effect of Mutation at S322 of Cytochrome b on the Rieske Iron−Sulfur Cluster. Figure 3 compares EPR spectra of the Rieske iron−sulfur cluster in complement and mutant complexes. When the complement complex was reduced with a slight excess of ascorbate, the EPR signals of the [2Fe-2S] cluster are at $g_x = 1.800$, $g_y = 1.898$, and $g_z = 2.026$, the same as previously reported for the wild-type complex (*16*). Under the same conditions, the cyt*b*-(S322A) mutant complex has g_y and g_z signals the same as those detected in the wild-type complex, but the g_x peak is broadened and shifts to $g = 1.768$. This indicates that alanine substitution at position 322 of cytochrome *b* perturbs the microenvironment of the [2Fe-2S] cluster of ISP. As expected, the broadened $g_x = 1.768$ signal is observed in mutant complexes of cyt*b*-Δ(309−326), cyt*b*-(309−326)A, and cyt*b*-(322−323)A (see Figure 3), since these mutant complexes lack the essential hydrogen bond forming hydroxyl group at residue 322.

Replacing S322 with T, Y, or C gives mutant complexes with EPR characteristics of the [2Fe-2S] cluster identical to those observed in the wild-type complex, indicating that the presence of a hydrogen bond forming residue at position 322 of cytochrome *b* is essential for maintaining proper microenvironments for the [2Fe-2S] cluster of ISP in the bacterial complex.

It has been reported that the g_x of ISP in bc_1 from *R. sphaeroides* is at $g = 1.800$ when ubiquinone is present but shifts to 1.750 and broadens when ubiquinol is present (*28*). When ubiquinone is extracted from chromatophore membranes, the g_x signal of the "depleted state" is at $g = 1.765$ and is considerably broader than those seen in the presence of either ubiquinone or ubiquinol. Although the broadened $g_x = 1.768$ resonance observed in the cyt*b*-(S322A) mutant complex resembles the "reduced state" or the "depleted state" spectrum, it is not because of changing the redox state of Q or a decrease of Q content in the mutant complex, because the EPR spectrum of the [2Fe-2S] cluster in this mutant complex is detected under the same redox conditions as with

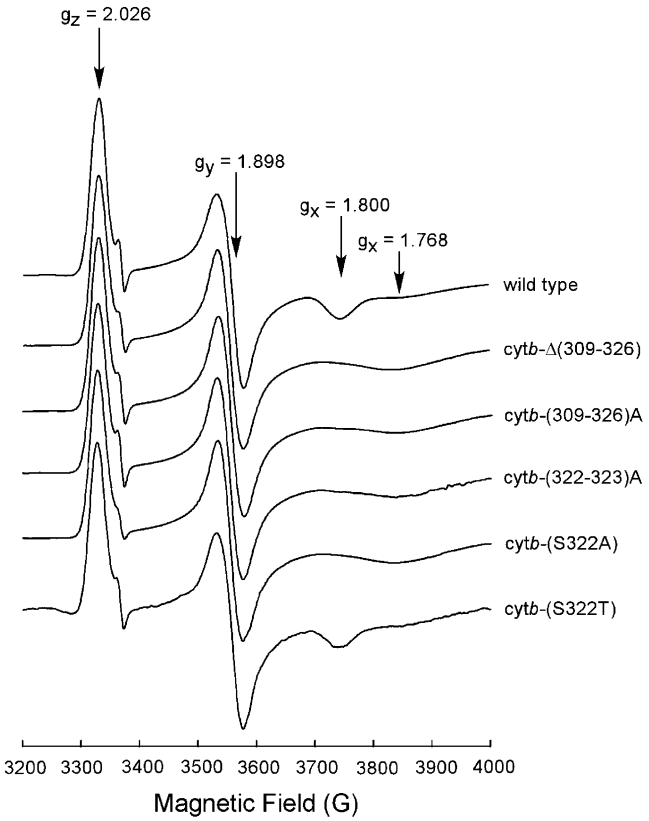

FIGURE 3: EPR spectra of the [2Fe-2S] cluster of the Rieske iron−sulfur protein in purified bc_1 complexes from the complement and mutants cyt*b*-Δ(309−326), cyt*b*-(309−326)A, cyt*b*-(322−323)A, cyt*b*-(S322A), and cyt*b*-(S322T). Purified complement and mutant bc_1 complexes were treated with a small excess of sodium ascorbate solution to fully reduce cytochrome c_1 and frozen in liquid nitrogen. EPR spectra were recorded at 11 K on a Bruker EMX EPR spectrometer equipped with an Air Products flow cryostat with the following instrument settings: microwave frequency, 9.3 GHz; microwave power, 2.2 mW; modulation amplitude, 6.3 G; modulation frequency, 100 kHz; time constant, 665.4 ms; sweep time, 167.8 s; conversion time, 163.8 ms.

the complement complex and the Q content in the cyt*b*-(S322A) mutant complex is the same as that in the complement complex.

The broadened $g_x = 1.768$ signal observed in the cyt*b*-(S322A) mutant complex is reminiscent of that observed for the substitution of Leu for Phe-144 (F144L) in cytochrome *b* from *R. capsulatus* (*29*) and of Ser for Thr-160 (T160S) in cytochrome *b* from *R. sphaeroides* (*16*). The F144L bc_1 complex in *R. capsulatus* and the T160S mutant complex in *R. sphaeroides* chromatophores were reported to have very low turnover rates with a broadened, redox state-insensitive, g_x value at 1.765. It was suggested that these properties of the F144L and T160S complexes resulted from a reduced affinity for quinone and quinol at the Q_o center of the mutant complexes. Since the apparent K_ms for $Q_0C_{10}BrH_2$ determined with mutant complexes of cyt*b*-Δ(309−326) and cyt*b*-(S322A) are 2.00 and 1.50 μM, respectively, which are comparable to that of the wild-type complex ($K_m = 1.56$ μM), mutational effects observed in a cyt*b*-(S322A) mutant complex cannot be attributed to a decrease in quinol binding at the Q_o site. The redox midpoint potentials of the [2Fe-2S] cluster in the complexes of wild type, cyt*b*-Δ(309−326), and cyt*b*-(S322A) are measured using circular dichroism (CD) spectroscopy on a Jasco J-715 spectropolarimeter, and the values are 231 ± 7, 224 ± 10, and 219 ± 8 mV, respectively. Because the redox potentials are similar, the loss of activity in the mutants cannot be attributed to a change of the redox potential of ISP.

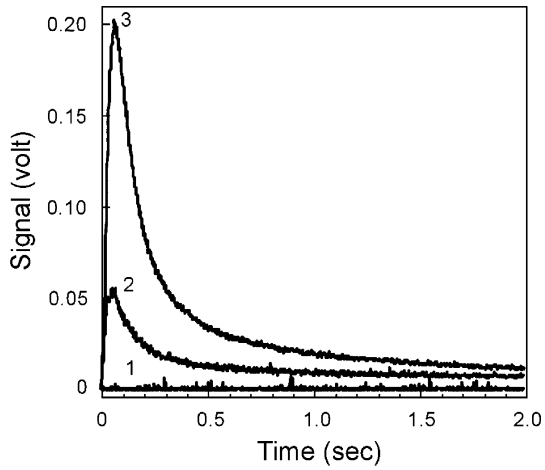

FIGURE 4: Tracings of superoxide generation in complement and mutant cyt*b*-(S322A) cytochrome bc_1 complexes. To measure the superoxide anion production during the pre-steady-state reaction of the reduction of the bc_1 complex by ubiquinol, stopped-flow assays were carried out at 23 °C in an Applied Photophysics stopped-flow reaction analyzer, SX 18MV, by mixing 1:1 solutions A and B. Solution A consisted of 100 mM Na^+/K^+ phosphate buffer, pH 7.4, containing 1 mM EDTA, 1 mM KCN, 1 mM NaN_3, 0.1% BSA, 0.01% DM, and 9 μM bc_1 complexes. Solution B was the same as solution A except that the bc_1 complex was replaced with 50 μM $Q_0C_{10}BrH_2$ and 4 μM MCLA. For each sample, eight kinetic traces were averaged. For control, either bc_1 complexes or $Q_0C_{10}BrH_2$ were omitted from the above system, or 300 units/mL SOD was added to the system. Tracings 1, 2, and 3 represent the control, the complement complex, and the cyt*b*-(S322A) mutant complex, respectively.

Since S322 is at the tip of this extra fragment of cytochrome *b* (D. Xia, privileged communication), which is located between the amphipathic helix *ef*, a key structural component of the Q_o site, and the transmembrane helix F, it is likely that the decreased turnover rate of the cyt*b*-(S322A) mutant complex is due to the weakening of the putative interaction between ISP and cytochrome *b* through the loss the hydroxyl group of S322. The high-field shift of the g_x EPR signal of S322A also indicates that some environment change of the 2Fe2S cluster might have occurred upon the loss of the hydroxyl group. Whether or not hydrogen bonding is involved in such an interaction is a question that cannot be answered until a high-resolution structure is available. The weakening interaction between cytochrome *b* and ISP may result in some conformational change at the Q_o site and thus enhances electron leakage to decrease the bc_1 activity.

Superoxide Anion Generation by the S322A Mutant Cytochrome bc_1 Complex. If the decrease in bc_1 activity observed in the cyt*b*-(S322A) mutant complex indeed results from increased electron leakage at the altered Q_o site, one would expect to see an increase in the rate of $O_2^{\bullet-}$ generation by this mutant complex, compared to that of the wild-type complex.

Figure 4 shows tracings of superoxide generation by wild-type and cyt*b*-(S322A) mutant bc_1 complexes. The rate of superoxide generation by the bc_1 complex was measured for the chemiluminescence of the MCLA−$O_2^{\bullet-}$ adduct during a single turnover of the bc_1 complex (in the absence of

Table 3: Production of Superoxide Anion by Purified Wild Type and Mutant Complexes

strain	superoxide anion (XO unit/mg of protein)[a]
wild type	0.19 ± 0.02
cyt*b*-Δ(309−326)	0.73 ± 0.03
cyt*b*-(309−326)A	0.72 ± 0.03
cyt*b*-(322−323)A	0.72 ± 0.02
cyt*b*-(S322A)	0.72 ± 0.02
cyt*b*-(F323A)	0.19 ± 0.03
cyt*b*-(S322T)	0.18 ± 0.03

[a] XO units are defined under Experimental Procedures. For the experimental conditions, see the legend to Figure 4. The data presented were mean values ± SD from five experiments.

cytochrome *c*) using the Applied Photophysics stopped-flow reaction analyzer SX.18 MV. Since the assay system contains no cytochrome *c*, chemiluminescence of MCLA−$O_2^{\bullet-}$ resulting from nonenzymatic oxidation of ubiquinol by cytochrome *c* is eliminated. MCLA chemiluminescence induced by the bc_1 complex reaches peak intensities after approximately 0.06 s at room temperature and then decays. No luminescence is detected when the bc_1 complex is omitted from the enzyme-containing solution or $Q_0C_{10}BrH_2$ is omitted from the substrate-containing solution (see the control in Figure 4). Addition of superoxide dismutase to either the substrate or enzyme solution completely abolishes luminescence (see the control in Figure 4), indicating that $O_2^{\bullet-}$ is responsible for the luminescence observed. Maximum peak height induced by the cyt*b*-(S322A) mutant complex is about four times that of the wild-type complex.

Table 3 compares the rates of $O_2^{\bullet-}$ generation by the wild-type and mutant cytochrome bc_1 complexes. Oxidation of ubiquinol by wild-type and cyt*b*-(S322A) mutant complexes produces 0.19 and 0.72 XO units of $O_2^{\bullet-}$/mg of protein, respectively. A similar increase in the rate of $O_2^{\bullet-}$ production is observed in mutant complexes of cyt*b*-Δ(309−326), cyt*b*-(309−326)A, cyt*b*-(322−323)A, and cyt*b*-(S322A). However, the rate of $O_2^{\bullet-}$ production by mutant complexes of cyt*b*-(F323A) and cyt*b*-(S322T) is similar to that of the wild-type complex. These results support the idea that alanine substitution at S322 causes conformational changes at the Q_o site, mainly through weakening of the interaction between ISP and cytochrome *b* due to a loss of the hydroxyl group at position 322. Substituting S322 with threonine does not alter the putative hydrogen bounding and therefore has no effect on superoxide generation and the bc_1 activity.

Effect of Mutation on the Thermotropic Properties of the Cytochrome bc_1 Complex. Since it has been shown that alanine substitution at S322 of cytochrome *b* decreases bc_1 complex activity, perturbs the microenvironment of ISP, and increases the rate of superoxide generation, it is of interest to see whether or not this mutation also affects the structural stability of the bc_1 complex. Differential scanning calorimetry (DSC), a widely used method for determining protein structural stability, was employed to compare the stability of wild-type and mutant complexes.

When the thermotrophic properties of wild-type and mutant cyt*b*-(S322A) complexes were measured by DSC, the mutant complex exhibited a thermodenaturation temperature (T_m) of 44.1 °C with an enthalpy change (ΔH) of 74.0 kcal/mol whereas the wild-type complex showed a T_m of 46.3 °C with a ΔH of 96.7 kcal/mol. Under identical conditions, mutant complexes of cyt*b*-Δ(309−326), cyt*b*-(309−326)A, cyt*b*-(S322T), cyt*b*-(S322Y), cyt*b*-(S322C), cyt*b*-(S322V), cyt*b*-(S322L), cyt*b*-(S322I), and cyt*b*-(S322F) showed T_ms of 43.3, 43.2, 46.2, 46.5, 46.1, 44.3, 44.3, 44.2, and 44.1 °C with ΔHs of 64.1, 63.6, 95.6, 96.9, 95.8, 74.5, 74.7, 74.3, and 73.8 kcal/mol, respectively. The lower T_m and ΔH of the mutant complex indicate that it is less stable than the wild-type complex. These results indicate that replacing the hydroxyl group bearing an amino acid residue at position 322 of cytochrome *b* with a non-hydroxyl amino acid causes a decrease not only in the electron transfer activity but also in the structural stability of the bc_1 complex.

ACKNOWLEDGMENT

We thank Dr. Roger Koeppe for critical review of the manuscript.

REFERENCES

1. Snyder, C., and Trumpower, B. L. (1998) Mechanism of ubiquinol oxidation by the cytochrome bc_1 complex: pre-steady-state kinetics of cytochrome bc_1 complexes containing site-directed mutants of the Rieske iron-sulfur protein, *Biochim. Biophys. Acta 1365*, 125−134.
2. Ljungdahl, P. O., Pennoyer, J. D., Robertson, D. E., and Trumpower, B. L. (1987) Purification of highly active cytochrome bc_1 complexes from phylogenetically diverse species by a single chromatographic procedure, *Biochim. Biophys. Acta 891*, 227−241.
3. Yang, X. H., and Trumpower, B. L. (1988) Protonmotive Q cycle pathway of electron transfer and energy transduction in the three-subunit ubiquinol-cytochrome *c* oxidoreductase complex of *Paracoccus denitrificans*, *J. Biol. Chem. 263*, 11962−11970.
4. Yu, L., Tso, S. C., Shenoy, S. K., Quinn, B. N., and Xia, D. (1999) The role of the supernumerary subunit of *Rhodobacter sphaeroides* cytochrome bc_1 complex, *J. Bioenerg. Biomembr. 31*, 251−257.
5. Berry, E. A., Huang, L. S., Saechao, L. K., Pon, N. G., Valkova-Valchanova, M., and Daldal, F. (2004) X-Ray structure of *Rhodobacter capsulatus* cytochrome bc_1: comparison with its mitochondrial and chloroplast counterparts, *Photosynth. Res. 81*, 251−275.
6. Xiao, K., Liu, X., Yu, C. A., and Yu, L. (2004) The extra fragment of the iron-sulfur protein (residues 96-107) of *Rhodobacter sphaeroides* cytochrome bc_1 complex is required for protein stability, *Biochemistry 43*, 1488−1495.
7. Liu, X., Yu, C. A., and Yu, L. (2004) The role of extra fragment at the C-terminal of cytochrome *b* (residues 421-445) in the cytochrome bc_1 complex from *Rhodobacter sphaeroides*, *J. Biol. Chem. 279*, 47363−47371.
8. Mitchell, P. (1976) Possible molecular mechanisms of the protonmotive function of cytochrome systems, *J. Theor. Biol. 62*, 327−367.
9. Turrens, J. F., Alexandre, A., and Lehninger, A. L. (1985) Ubisemiquinone is the electron donor for superoxide formation by complex III of heart mitochondria, *Arch. Biochem. Biophys. 237*, 408−414.
10. Nohl, H., and Jordan, W. (1986) The mitochondrial site of superoxide formation, *Biochem. Biophys. Res. Commun. 138*, 533−539.
11. Zhang, L., Yu, L., and Yu, C. A. (1998) Generation of superoxide anion by succinate-cytochrome *c* reductase from bovine heart mitochondria, *J. Biol. Chem. 273*, 33972−33976.
12. Muller, F., Crofts, A. R., and Kramer, D. M. (2002) Multiple Q-cycle bypass reactions at the Qo site of the cytochrome bc_1 complex, *Biochemistry 41*, 7866−7874.
13. Sun, J., and Trumpower, B. L. (2003) Superoxide anion generation by the cytochrome bc_1 complex, *Arch. Biochem. Biophys. 419*, 198−206.
14. Yu, C. A., and Yu, L. (1982) Syntheses of biologically active ubiquinone derivatives, *Biochemistry 21*, 4096−4101.
15. Khosravi, M., Ryan, W., Webster, D. A., and Stark, B. C. (1990) Variation of oxygen requirement with plasmid size in recombinant *Escherichia coli*, *Plasmid 23*, 138−143.

16. Mather, M. W., Yu, L., and Yu, C. A. (1995) The involvement of threonine 160 of cytochrome *b* of *Rhodobacter sphaeroides* cytochrome bc_1 complex in quinone binding and interaction with subunit IV, *J. Biol. Chem. 270*, 28668−28675.
17. Tian, H., Yu, L., Mather, M. W., and Yu, C. A. (1998) Flexibility of the neck region of the Rieske iron-sulfur protein is functionally important in the cytochrome bc_1 complex, *J. Biol. Chem. 273*, 27953−27959.
18. Berden, J. A., and Slater, E. C. (1970) The reaction of antimycin with a cytochrome *b* preparation active in reconstitution of the respiratory chain, *Biochim. Biophys. Acta 216*, 237−249.
19. Yu, L., Dong, J. H., and Yu, C. A. (1986) Characterization of purified cytochrome c_1 from *Rhodobacter sphaeroides* R-26, *Biochim. Biophys. Acta 852*, 203−211.
20. Gong, X., Yu, L., Xia, D., and Yu, C. A. (2005) Evidence for electron equilibrium between the two hemes b_L in the dimeric cytochrome bc_1 complex, *J. Biol. Chem. 280*, 9251−9257.
21. Redfearn, E. R. (1967) Isolation and determination of ubiquinone, *Methods Enzymol. 10*, 381−384.
22. Lowry, O. H., Rosebrough, N. J., Farr, A. L., and Randall, R. J. (1951) Protein measurement with the Folin phenol reagent, *J. Biol. Chem. 193*, 265−275.
23. Laemmli, U. K. (1970) Cleavage of structural proteins during the assembly of the head of bacteriophage T4, *Nature 227*, 680−685.
24. Dutton, P. L. (1978) Redox potentiometry: determination of midpoint potentials of oxidation-reduction components of biological electron-transfer systems, *Methods Enzymol. 54*, 411−435.
25. Guner, S., Robertson, D. E., Yu, L., Qiu, Z. H., Yu, C. A., and Knaff, D. B. (1991) The *Rhodospirillum rubrum* cytochrome bc_1 complex: redox properties, inhibitor sensitivity and proton pumping, *Biochim. Biophys. Acta 1058*, 269−279.
26. Link, T. A., Hatzfeld, O. M., Unalkat, P., Shergill, J. K., Cammack, R., and Mason, J. R. (1996) Comparison of the "Rieske" [2Fe-2S] center in the bc_1 complex and in bacterial dioxygenases by circular dichroism spectroscopy and cyclic voltammetry, *Biochemistry 35*, 7546−7552.
27. Ugulava, N. B., and Crofts, A. R. (1998) CD-monitored redox titration of the Rieske Fe-S protein of *Rhodobacter sphaeroides*: pH dependence of the midpoint potential in isolated bc_1 complex and in membranes, *FEBS Lett. 440*, 409−413.
28. McCurley, J. P., Miki, T., Yu, L., and Yu, C. A. (1990) EPR characterization of the cytochrome bc_1 complex from *Rhodobacter sphaeroides*, *Biochim. Biophys. Acta 1020*, 176−186.
29. Robertson, D. E., Daldal, F., and Dutton, P. L. (1990) Mutants of ubiquinol-cytochrome c_2 oxidoreductase resistant to Qo site inhibitors: consequences for ubiquinone and ubiquinol affinity and catalysis, *Biochemistry 29*, 11249−11260.

BI061099A